confirms the fact that C^{**}_{coil} is independent of molecular weight. In order to compare with available experimental data, the overlap concentrations between dilute and semidilute regimes and the crossover concentrations between semidilute and concentrated regimes were computed according to eq 6, 9, 18, and 40. The results are listed in Table III.

In comparing our approach with experiments, it should be emphasized that experimental values for the overlap concentrations are very difficult to obtain, especially for C^{**}. We have some confidence in our own experimental estimates for poly(1,4-phenyleneterephthalamide) (PPTA) in concentrated sulfuric acid and polystyrene (PS) in *trans*-decalin. Using forced Rayleigh light-scattering methods, Leger and co-workers[7] reported C^* values for the PS–benzene system (except the value of C^* of the highest molecular weight sample $M_w = 7.54 \times 10^5$, which was estimated from Figure 5 in ref 7), which are in very good agreement with the calculated C^* values. The xanthan results are rough approximations and are included to provide additional experimental evidence. As the values of persistence length of xanthan from the literature[13,21] were either estimated or calculated from the Kuhn statistical length, three different C^{**}_{calcd} values, as listed in Table III, could be presented. Nevertheless, the C^{**}_{calcd} values are within, or close to, the range of experimental estimates reported. The same predictions for the poly(γ-benzyl L-glutamate) (PBLG)–1,2-dichloroethane system are shown in Table III, where we have used two different ρ values (140 and 90 mn) to compute the C^{**}_{calcd} values, while $C^{**}_{exptl} \sim 5 \times 10^3$ g/mL for $M_w \sim 1.5 \times 10^5$. The overall agreement between experiment and theory is indeed remarkable. Further confirmation awaits additional experimental data.

Conclusions

Overlap and crossover concentrations (C^* and C^{**}) are geometric problems controlled merely by effective volumes, irrespective of particle shape. If we take the persistence length as a fundamental parameter and assume that the molecular volume remains a constant, independent of chain flexibility, we can then correlate the overlap crossover concentrations from random coils to rigid rods with the effective length $L^* \simeq (\rho L)^{1/2}$ and the effective diameter $d^* \simeq (L/\rho)^{1/4} d$ for wormlike chains.

Acknowledgment. We gratefully acknowledge support of this research by the National Science Foundation (Grant Nos. DMR 8314193 and INT8211992).

Registry No. PS, 9003-53-6; PPTA (SRU), 24938-64-5; PPTA (copolymer), 25035-37-4; PBLG (SRU), 25038-53-3; PBLG (homopolymer), 25014-27-1; xanthan, 11138-66-2.

References and Notes

(1) Graessley, W. W. *Adv. Polym. Sci.* **1974**, *16*, 1.
(2) Berry, G. C.; Nakayasu, H.; Fox, T. G. *J. Polym. Sci., Polym. Phys. Ed.* **1979**, *17*, 1825.
(3) Daoud, M.; Cotton, J. P.; Farnoux, B.; Jannink, G.; Sarma, G.; Benoit, H.; Duplessix, R.; Picot, C.; de Gennes, P.-G. *Macromolecules* **1975**, *8*, 804.
(4) Cotton, J. P.; Nierlich, M.; Boue, F.; Daoud, M.; Farnoux, B.; Jannink, G.; Duplessix, R.; Picot, C. *J. Chem. Phys.* **1976**, *65*, 1101.
(5) Graessley, W. W. *Polymer* **1980**, *21*, 258.
(6) Doi, M.; Edwards, S. F. *J. Chem. Soc., Faraday Trans. 2* **1978**, *74*, 560, 918.
(7) Leger, L.; Hervet, H.; Rondelez, R. *Macromolecules* **1981**, *14*, 1732.
(8) Maguire, J. F.; McTague, J. P. *Phys. Rev. Lett.* **1980**, *45*, 1891.
(9) Ying, Q.; Chu, B.; Qian, R.; Bao, J.; Zhang, J.; Xu, C. *Polymer* **1985**, *26*, 1401.
(10) Zero, K. M.; Pecora, R. *Macromolecules* **1982**, *15*, 87.
(11) Kubota, K.; Chu, B. *Biopolymer* **1983**, *22*, 1461.
(12) Ying, Q.; Chu, B. *Macromolecules* **1986**, *19*, 1580.
(13) Southwick, J. G.; Jamieson, A. M.; Blackwell, J. *Macromolecules* **1981**, *14*, 1728.
(14) Jain, S.; Cohen, C. *Macromolecules* **1981**, *14*, 759.
(15) Odijk, J. *Macromolecules* **1983**, *16*, 1340.
(16) Flory, P. J.; Fox, T. G., Jr. *J. Am. Chem. Soc.* **1951**, *73*, 1904.
(17) Yamakawa, H.; Fujii, M. *Macromolecules* **1974**, *7*, 128.
(18) Flory, P. J. *Principles of Polymer Chemistry*; Cornell University: Ithaca, NY, 1953; Chapter XIV, p 606.
(19) Nemoto, N.; Landry, M. R.; Noh, I.; Kitano, T.; Wesson, J. A.; Yu, H. *Macromolecules* **1985**, *18*, 308.
(20) Flory, P. J. *Principles of Polymer Chemistry*; Cornell University: Ithaca, NY, 1953; Chapter X, p 413.
(21) Jamieson, A. M. *Polym. Prepr. (Am. Chem. Soc., Div. Polym. Chem.)* **1982**, *23*(1), 69.
(22) Aharoni, S. M. *Macromolecules* **1983**, *16*, 1722.
(23) Hervet, G.; Leger, L.; Rondelez, R. *Phys. Rev. Lett.* **1979**, *42*, 1681.
(24) Chu, B.; Nose, T. *Macromolecules* **1979**, *12*, 599.

Self-Consistent Field Theory for the Adsorption of Ring Polymers from Solution

Boudewijn van Lent, Jan Scheutjens, and Terence Cosgrove*

Laboratory for Physical Chemistry, Agricultural University, De Dreijen 6, 6703 BC Wageningen, The Netherlands. *Received August 27, 1986*

ABSTRACT: The self-consistent field polymer adsorption theory of Scheutjens and Fleer has been extended for the case of ring macromolecules. This is achieved by enumerating the chain conformations in three dimensions while maintaining a mean field approximation to calculate the different interaction enthalpies. A comparison of the adsorption of rings and linear chains shows that under certain physical conditions the adsorbed amount of rings is higher, whereas in other cases the reverse is true. The volume fraction of segments in trains and loops is calculated as are the RMS thickness and bound fractions for different values of the adsorption energy and for a variety of different solvency conditions.

Introduction

One of the most interesting phenomena in the adsorption of polymers at the solid–solution interface is the prediction that segments of adsorbed molecules can exist in extended "tails".[1] The Scheutjens–Fleer theory,[2,3] in particular, predicts that at high adsorbed amounts very long tails are formed. This prediction has been corroborated experimentally by hydrodynamic thickness measurements.[4,5]

One way of investigating the influence of tails on adsorption properties is to study a system that only has segments in loops and trains. An ideal system from this

*School of Chemistry, University of Bristol, Cantock's Close, Bristol BS8 1TS, U.K.

0024-9297/87/2220-0366$01.50/0

point of view is one consisting of polymer rings. These molecules can be prepared in narrow molecular weight fractions and at reasonably high degrees of polymerization, typically 200–300 monomers.[6] Although some of the solution properties of these polymers are known,[7,8] no experimental or theoretical data regarding their adsorption properties have been given. In this paper we extend the Scheutjens–Fleer theory for the case of the adsorption of ring polymers. Experimental data on the adsorption properties of these systems will be published separately.

Theory

The Scheutjens–Fleer (SF) theory[2,3] is an extension of the Flory–Huggins lattice model of polymer solutions. In the adsorption model the lattice consists of layers parallel to the surface, numbered 1–M. Layer 1 is the layer next to the surface, while layer M is in the bulk solution. A site on the lattice has z nearest neighbors of which a fraction λ_0 is in the same layer and a fraction λ_1 is in each of the adjacent layers, i.e., $\lambda_0 + 2\lambda_1 = 1$. A lattice site can be occupied by a solvent molecule or a polymer segment. Ignoring free volume effects, we have

$$\phi_i + \phi_i^0 = 1 \tag{1}$$

where ϕ_i is the volume fraction of polymer segments and ϕ_i^0 the volume fraction of solvent molecules in layer i. The volume fractions in the bulk solution are ϕ_* and ϕ_*^0, respectively.

A very important parameter in the theory is the free segment probability p_i. This is a Boltzmann weighting factor which determines the probability that a "free" monomer is in layer i relative to the bulk solution. For the bulk solution $p_i = p_* = 1$. If p_i is greater than 1, the free monomer is more likely to occur in layer i than in the bulk solution. p_i is given by

$$p_i = (\phi_i^0/\phi_*^0)e^{2\chi(\langle\phi_i\rangle-\phi_*)}e^{(\chi_s+\lambda_1\chi)\delta(1,i)} \tag{2}$$

The factor ϕ_i^0/ϕ_*^0 arises from the difference in solvent configurational entropy between the bulk and layer i.

The difference in interaction energy between a segment in layer i and in the bulk is accounted for in the term $2\chi(\langle\phi_i\rangle - \phi_*)$, where χ is the Flory–Huggins interaction parameter and $\langle\phi_i\rangle$ is the site volume fraction defined by

$$\langle\phi_i\rangle = \lambda_1\phi_{i-1} + \lambda_0\phi_i + \lambda_1\phi_{i+1} \tag{3}$$

The factor $e^{(\chi_s+\lambda_1\chi)\delta(1,i)}$ takes the effect of the adsorption energy into account and $\delta(1,i)$ is the Kronecker delta, which equals 1 when $i = 1$ but otherwise equals 0. The adsorption energy parameter, χ_s, is the difference in energy (kT) of the adsorption of a segment and a solvent molecule.[9] The term $\lambda_1\chi$ in the exponent arises because a segment in the first layer has exchanged $\lambda_1 z$ contacts in the solution for the same number of surface contacts.

For a linear polymer the probability of finding a segment in a given layer depends on its position in the chain. However, for a ring polymer this condition is relaxed; the segments are indistinguishable and contribute equally to the volume fraction in each layer. Note that this is the same condition that Roe[10] uses as a simplification in his theory on the adsorption of linear chains. Therefore

$$\phi_i = r\phi(i,1) \tag{4}$$

where $\phi(i,1)$ is the volume fraction in layer i due to an arbitrary segment "one" and r is the number of segments in the ring. For a complete ring, $\phi(i,1)$ is found by calculating the probability of all possible conformations having segment 1 in a lattice site in layer i with segment r in an adjacent site. This can only be achieved by enumerating the chain conformations in three dimensions; otherwise, conformations will be included with their first and last segment in the same or an adjoining layer, but not necessarily in an adjacent lattice site.

We start with extending the matrix method developed by DiMarzio and Rubin[11] into three dimensions. This method will give the end-segment probability $p_i(j,k,l;r)$ of a linear chain of r segments, i.e., the probability that the end segment of a chain of r segments ends in layer j in the site with coordinates k and l while the first segment is in site $(i,0,0)$.

Placing the first segment in site $(i,0,0)$ we find that the end-segment probability $p_i(i,0,0;1)$ of a "chain" of one segment equals the free segment probability p_i, whereas for every other lattice site $p_i(j,k,l;1)$ equals zero:

$$\begin{aligned} p_i(j,k,l;1) &= p_i \quad \text{if } j = i,\ k = 0, \text{ and } l = 0 \\ &= 0 \quad \text{if } j \neq i, \text{ or } k \neq 0, \text{ or } l \neq 0 \end{aligned} \tag{5}$$

Note that the free segment probability p_i depends only on the layer number i.

From the end-segment probabilities $p_i(j,k,l;1)$ it is possible to calculate the end-segment probabilities for a chain of two segments. For a cubic lattice we find

$$\begin{aligned} p_i(j,k,l;2) = [&p_i(j-1,k,l;1) + p_i(j+1,k,l;1) + p_i(j,k-1,l;1) \\ &+ p_i(j,k+1,l;1) + p_i(j,k,l-1;1) + p_i(j,k,l+1;1)]p_j/6 \end{aligned} \tag{6}$$

where p_j is the free segment probability for layer j. Obviously, for other lattice types a similar equation can be given. For a lattice with coordination number z there will be a sum of z end-segment probabilities at the right-hand side of eq 6. For a cubic lattice there are, of course, only six combinations of j, k, and l that give us a nonzero $p_i(j,k,l;2)$. In the same way the end-segment probabilities of a chain of three segments can be found from the end-segment probabilities of a chain of two segments and so on. In general we can write (for a cubic lattice and if step reversals are allowed)

$$\begin{aligned} p_i(j,k,l;r) = \\ [&p_i(j-1,k,l;r-1) + p_i(j+1,k,l;r-1) + p_i(j,k-1,l;r-1) + \\ &p_i(j,k+1,l;r-1) + p_i(j,k,l-1;r-1) + p_i(j,k,l+1;r-1)]p_j/6 \end{aligned} \tag{7}$$

The volume fraction $\phi(i,1)$, used in eq 4, can then be calculated from these end-segment probabilities as follows. For every j we calculate the value of $\phi_i(j,s)$, which is the contribution of segment s to the volume fraction in layer j, while the first segment is in layer i. If a number of conformations have segment s in layer j and segment 1 in layer i, we know that the contribution of their segment s to the volume fraction in layer j is the same as the contribution of their segment 1 to the volume fraction in layer i. Hence

$$\phi(i,1) = \sum_j \phi_i(j,s) \tag{8}$$

Note that s can be chosen arbitrarily. We can obtain $\phi_i(j,s)$ from

$$\phi_i(j,s) = C\sum_{k,l} p_i(j,k,l;s,r) \tag{9}$$

C is a normalization factor and $p_i(j,k,l;s,r)$ is the probability of finding the sth segment of a ring polymer with chain length r in lattice site (j,k,l) while segment 1 is in site $(i,0,0)$. To calculate $p_i(j,k,l;s,r)$ we join two chains of s and $r-s+2$ segments, respectively. Both have their first segment in site $(i,0,0)$ and their last in site (j,k,l). Hence we find

$$p_i(j,k,l;s,r) = \frac{p_i(j,k,l;s)p_i(j,k,l;r-s+2)}{p_i p_j} \tag{10}$$

In eq 10 we must divide by p_i and p_j because they are

included in both end-segment probabilities. Combining of eq 4, 8, 9, and 10 gives

$$\phi_i = rC\sum_{j,k,l}\frac{p_i(j,k,l;s)p_i(j,k,l;r-s+2)}{p_ip_j} \quad (11)$$

Now we must find an expression for the normalization factor C. For the bulk solution eq 11 becomes

$$\phi_* = rC\sum_{j,k,l}p_*(j,k,l;s)p_*(j,k,l;r-s+2)$$

Hence

$$C = \phi_*/rc_* \quad (12)$$

where

$$c_* = \sum_{j,k,l}p_*(j,k,l;s)p_*(j,k,l;r-s+2) \quad (13)$$

The quantities $p_*(j,k,l;s)$ can be found by substituting in eq 7 that $p_j = 1$ for every j. Comparison with the normalization constant for linear chains (ref 2, eq 45) shows that c_* compensates for the reduction in conformational entropy of the rings in bulk solution.

Combination of eq 11 and 12 yields the final expression for ϕ_i:

$$\phi_i = \frac{\phi_*}{c_*}\sum_{j,k,l}\frac{p_i(j,k,l;s)p_i(j,k,l;r-s+2)}{p_ip_j} \quad (14)$$

Note that for $s = 1$ substitution of eq 5 simplifies eq 13 and 14 drastically. However, the best choice for s is the value $r/2$, because then only end-segment probabilities up to $s = r/2$ are to be computed.

When eq 1, 2, and 14 are used, the concentration profiles for adsorbed rings can be found by a numerical minimization procedure.[2]

In order to calculate the volume fractions due to adsorbed rings, ϕ_i^a, we must subtract the volume fraction of free chains, ϕ_i^f, from ϕ_i.[2] These volume fractions of free chains are directly obtained from eq 5, 7, and 14 by using $p_1 = 0$. Note that for ring polymers the volume fraction due to segments in loops, ϕ_i^l, equals ϕ_i^a $(i > 1)$.

Method of Computation

In practice we do not have to calculate all the end-segment probabilities $p_i(j,k,l;s)$, as there is a high degree of symmetry in the cubic lattice in the k and l directions. For all end-segment probabilities the following expression is valid:

$$p_i(j,k,l;s) = p_i(j,-k,l;s) = p_i(j,k,-l;s) = p_i(j,-k,-l;s) = p_i(j,l,k;s) = p_i(j,-l,k;s) = p_i(j,l,-k;s) = p_i(j,-l,-k;s) \quad (15)$$

This means that for each value of j in eq 9 we need only values of $p_i(j,k,l;s,r)$ in the first quadrant in the area between and including the lines $l = 0$ and $k = l$. To find $\phi_i(j,s)$ we have to multiply $p_i(j,k,l;s,r)$ by 8 for the values of k and l within the boundaries. For the boundaries themselves, the lines $l = 0$ and $k = l$, we must multiply by 4 except for the point $(j,0,0)$.

Results and Discussion

In Figure 1a,b we show concentration profiles for ring polymers of chain length 30 and for linear chains of the same length. The profiles are given for good solvent conditions ($\chi = 0$), a bulk concentration $\phi_* = 10^{-4}$, and two values of χ_s. For both values of χ_s, the linear chains extend further into solution than the rings, as expected, even though the adsorbed amounts are similar. In each inset we show expanded profiles, from layer 4 up to layer 8, which highlight this difference. As the hydrodynamic thickness of the adsorbed layer is determined by segments in the periphery of the profile,[4] it is clear that measurements of this kind would be very useful in comparing adsorbed rings and linear molecules. In Figure 1b we see that for $\chi_s = 0.5$ the adsorbed amount for rings is greater than that for the linear chains, whereas the reverse is true for $\chi_s = 3$ (Figure 1a, inset). This difference is seen more clearly in Figures 2 and 3. In Figure 2, the variation of the adsorbed amount $\theta = \sum\phi_i^a$ with χ_s is shown, and in Figure 3 we give adsorption isotherms. In Figure 3 there is a crossover around $\chi_s = 2.2$ for $\chi = 0.5$ but at a larger value of χ_s ($\sim$2.7) for $\chi = 0$. However, both crossovers appear to occur for similar values of θ. This emphasizes again the importance of the adsorbed amount in determining the structure of the adsorbed layer. In Figure 3 a similar effect is seen in the adsorption isotherms, the crossover occurring at a lower value of ϕ_* for the higher χ_s. The crossover, however, is not seen for $\chi_s = 1$ in the range of ϕ_* shown. The data are shown for very short molecules because of the large computation times required, but it is anticipated that these effects should be more marked for higher molecular weights. The crossover effects can be understood since at low coverage the difference in conformational entropy loss on adsorption between rings and linear chains favors the adsorption of rings, whereas at high adsorbed amounts the development of tails increases the adsorption of linear molecules. A ring loses less entropy on adsorption than a linear chain. However, the entropy difference *per segment* between rings and linear chains converges to zero in the limit of infinite chain length.[12] For infinite chain length the onset of adsorption

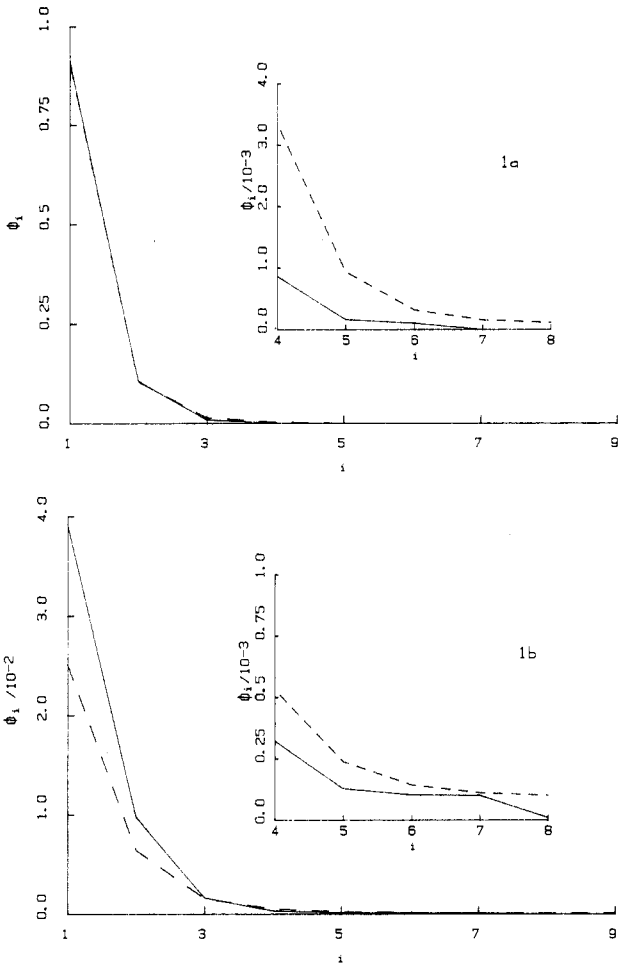

Figure 1. (a) Volume fraction ϕ_i as a function of layer number i for rings (—) and linear chains (- - -). The calculations are made for molecules of 30 segments in a good solvent ($\chi = 0$) on a cubic lattice and a bulk concentration $\phi_* = 10^{-4}$: $\chi_s = 3$. (b) As (a) but $\chi_s = 0.5$

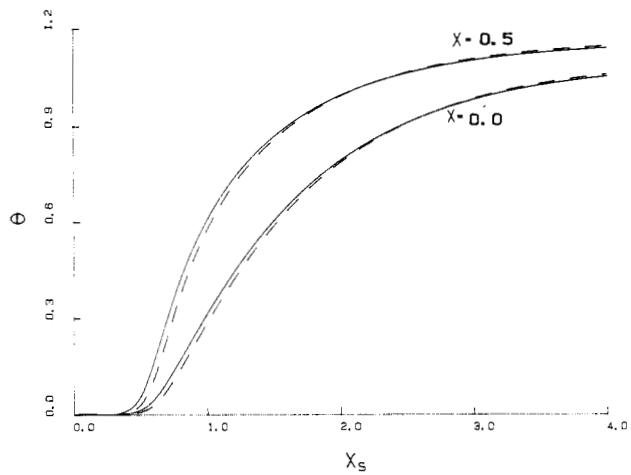

Figure 2. Adsorbed amount θ as a function of χ_s for rings (—) and linear chains (- - -) in a good solvent ($\chi = 0$) and in a Θ solvent ($\chi = 0.5$). $r = 20$ and $\phi_* = 10^{-4}$.

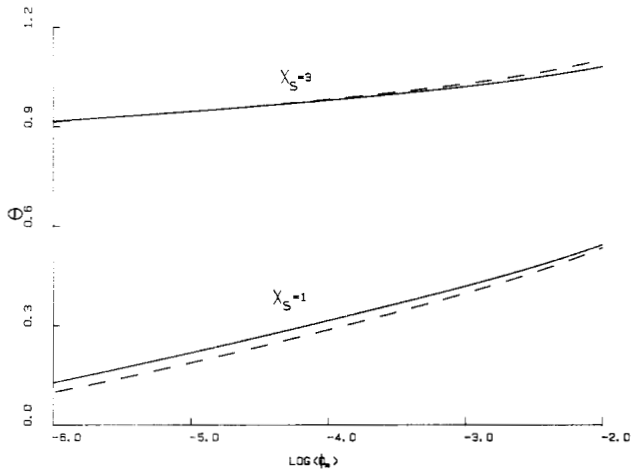

Figure 3. Adsorbed amount θ as a function of the bulk concentration for rings (—) and linear chains (- - -) in good solvent ($\chi = 0$) for $\chi_s = 1$ and for $\chi_s = 3$. $r = 20$.

occurs at a critical adsorption energy χ_{sc} that compensates the change in conformational entropy per segment. Hence χ_{sc} (which is 0.1823 for a cubic lattice) is the same for rings and linear chains. For finite chain lengths, however, the difference in conformational entropy per molecule gives rise to the onset of adsorption at different values of χ_s (see Figure 3).

In Figure 2 we also show the effect of changing solvency. The major effect of reducing solvency here is to increase the adsorbed amount for a given value of ϕ_*.

In Figure 4 we show the contributions from loops for the data in Figure 1. Rings clearly form more extended loops than linear chains for similar adsorbed amounts. In all cases the density of loops decays monotonically with distance from the surface.

In Figure 5 we compare the RMS layer thickness for rings and linear chains. The RMS layer thickness, t_{RMS}, is given by

$$t_{RMS}^2 = \sum_{i=1}^{M} \phi_i^a i^2 / \theta \qquad (16)$$

where ϕ_i^a is the volume fraction of adsorbed chains. In all cases, as expected, linear chains form thicker layers than rings, even at very low solution concentrations. An interesting observation is that the data for $\chi_s = 1$ predict thinner layers than for $\chi_s = 0.5$, even though the adsorbed amount is greater for the first case. This can be understood in that the probability of finding segments at larger distances from the interface is greater at low χ_s (see also Figure 1).

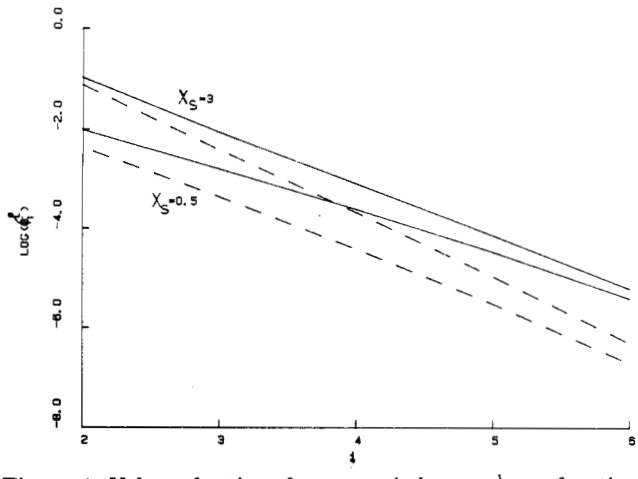

Figure 4. Volume fraction of segments in loops, ϕ_i^1, as a function of layer number i for rings (—) and linear chains (- - -) for the same parameters as in Figure 1.

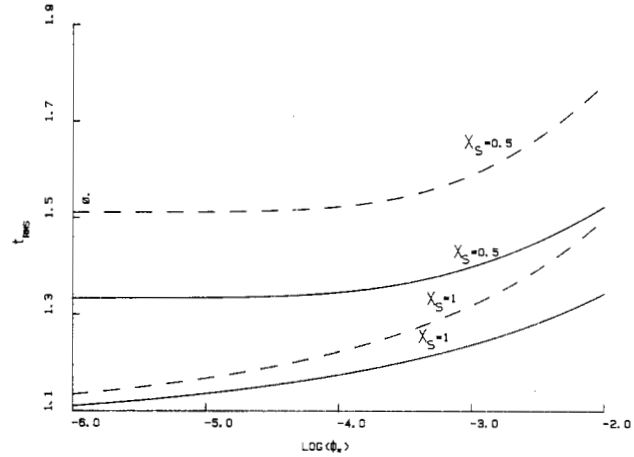

Figure 5. Root mean square layer thickness (t_{RMS}) as a function of the bulk concentration for rings (—) and linear chains (- - -) for $\chi_s = 0.5$ and for $\chi_s = 1$. $r = 20$ and $\chi = 0$.

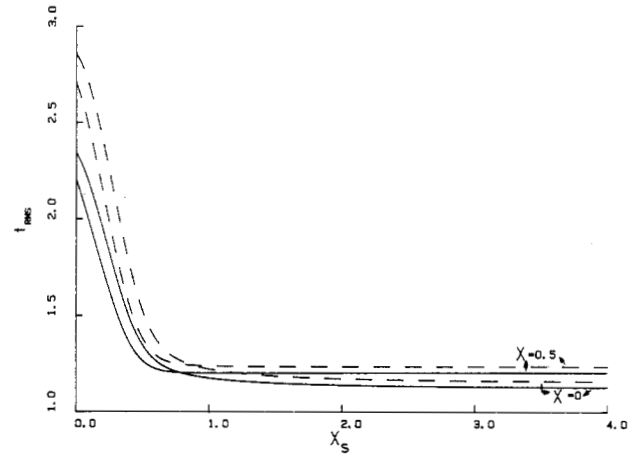

Figure 6. Root mean square layer thickness as a function of χ_s for rings (—) and linear chains (- - -) for a Θ solvent ($\chi = 0.5$) and a good solvent ($\chi = 0$). $r = 20$ and $\phi_* = 10^{-4}$.

Finally, in Figures 6 and 7 we show the variation in t_{RMS} and the bound fraction, $p = \phi_1/\theta$, with χ_s for different values of χ. For the depletion region ($\chi_s < \chi_{sc}$) the t_{RMS} value drops with increasing χ_s (and increasing adsorbed amount). There is a concomitant increase in p. With the same conditions, t_{RMS} of rings is always smaller than t_{RMS}

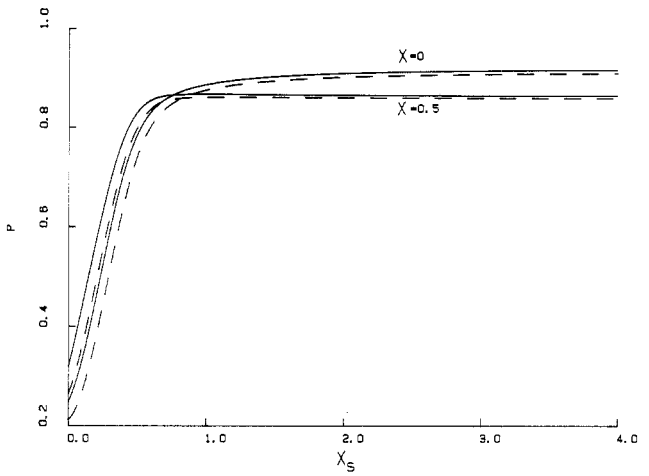

Figure 7. Bound fraction p as a function of χ_s for rings (—) and linear chains (- - -) for a Θ solvent ($\chi = 0.5$) and a good solvent ($\chi = 0$). $r = 20$ and $\phi_* = 10^{-4}$.

of linear chains and p of rings is always greater than p of linear chains. Polymer rings will be slightly more effectively anchored at an interface but will always form a thinner layer.

Conclusion

We have shown that the self-consistent field theory of Scheutjens and Fleer can be successfully adapted for the case of ring polymers. The results of these calculations emphasize the importance of tails in determining the adsorbed amount, the layer thickness, and the bound fraction.

Acknowledgment. We thank Timothy Heath, Brian Vincent, and Gerard Fleer for their continued interest and encouragement during this project.

References and Notes

(1) Cosgrove, T.; Vincent, B. *Adv. Colloid Interface Sci.* **1986**, *24*, 142.
(2) Scheutjens, J. M. H. M.; Fleer, G. J. *J. Phys. Chem.* **1979**, *83*, 1619.
(3) Scheutjens, J. M. H. M.; Fleer, G. J. *J. Phys. Chem.* **1980**, *84*, 178.
(4) Cohen Stuart, M. A.; Waajen, F. H. W. H.; Cosgrove, T.; Vincent, B.; Crowley, T. L. *Macromolecules* **1984**, *17*, 1825.
(5) Cosgrove, T.; Vincent, B.; Crowley, T. L.; Cohen Stuart, M. A. *ACS Symp. Ser.* **1984**, *240*, 147.
(6) Brown, J. F.; Slusarczuk, G. M. J. *J. Am. Chem. Soc.* **1965**, *87*, 931.
(7) Chen, Yi-Der *J. Chem. Phys.* **1981**, *74*, 2034.
(8) Higgins, J. S.; Ma, K.; Nicholson, L. K.; Hayter, J. B.; Dodgson, K.; Semlyen, J. A. *Polymer* **1983**, *24*, 793.
(9) Silberberg, A. *J. Chem. Phys.* **1968**, *48*, 2835.
(10) Roe, R. J. *J. Chem. Phys.* **1974**, *60*, 4192.
(11) DiMarzio, E. A.; Rubin, R. J.; *J. Chem. Phys.* **1971**, *55*, 4318.
(12) Whittington, S. G., private communication. Broadbent, S. R.; Hammersley, J. M. *Proc. Cambridge Philos. Soc.* **1957**, *53*, 629, 642.

Forward Depolarized Dynamic Light Scattering from Wormlike Chains

Sergio R. Aragón S.

Department of Chemistry, San Francisco State University, San Francisco, California 94132.
Received September 23, 1986

ABSTRACT: The forward depolarized light scattering correlation function is calculated for a dilute solution of polymers modeled as elastic wormlike chains in the free-draining limit. The polymer is represented hydrodynamically by an effective cylindrically symmetric body and characterized by a single end-over-end rotational diffusion coefficient, Θ. The correlation function for N polymer molecules is an infinite series of decaying exponentials of the form $C(t) = (N\beta^2/15)e^{-6\Theta t}\sum_{jk}a_{jk}b_{jk}(a)\exp[-D(x_j^4 + x_k^4)t/(2aL^2)]$, where β is the segment optical anisotropy, D is the translational diffusion coefficient, L is the contour length, and $a = \lambda L$ is the number of Kuhn lengths. The quantities $x_j \simeq (2j + 1)\pi/2$ are eigenvalues of the elastic bending problem. An important feature of the above result is the combination of rotational and flexural contributions to the time constants of the relaxation terms. The relative contribution of each of these processes is a function of flexibility. Comparison with Brownian dynamics simulations indicates that the weights are greatly affected by the neglect of hydrodynamic interactions in the theory. Nevertheless, this equation is the first calculation of the depolarized scattering from a semiflexible molecule that has the correct rigid rod limit. It should also be applicable for the description of the field-free decay of the birefringence from molecules without a permanent dipole moment. The theory is in good agreement with experimental data from DNA restriction fragments.

I. Introduction

The wormlike coil model of Kratky and Porod[1] is one of the simplest one-parameter descriptions available for stiff linear polymer chains. the attractiveness of the model stems from its ability to span the whole range of flexibilities from the random coil to the rigid rod. The properties of the polymer chain can be expressed in terms of the ratio, a, of the Kuhn statistical segment length, λ^{-1}, to the contour length, L. The persistence length, P, which is half the Kuhn length, is a commonly used alternative parameter. These parameters are related to the intrinsic chain elasticity parameter ϵ by $\lambda = kT/2\epsilon$. The transport and static properties of wormlike chain models have been reviewed recently by Yamakawa.[2] It is evident that the dynamics of these models is still in its development stage.

Harris and Hearst[3] were the first to propose a dynamical model of the wormlike chain treated as a differentiable space curve. This model has been criticized by Soda[4] for its internal inconsistencies. Nevertheless, it has been used in calculations of the forward depolarized dynamic scattering by Moro and Pecora[5] and extensively by Maeda and Fujime[6-8] to describe the polarized dynamic light scattering from semiflexible filaments. In a recent paper (hereafter referred to as I) Aragón and Pecora[9] presented a treatment of the dynamics of wormlike chains that is free of the inconsistencies of the Harris and Hearst model. By elim-

0024-9297/87/2220-0370$01.50/0